

A Tilt Model for Anomalous Cosmic Rays and the Location of the Solar Wind Termination Shock

E.C. Stone and A.C. Cummings

Space Radiation Laboratory, Caltech, MC 220-47, Pasadena, CA 91125, USA

Abstract

We use the observed relationship of the radial gradient of anomalous cosmic rays (ACRs), as measured in the outer heliosphere with instruments on the Voyager and Pioneer spacecraft, and the tilt of the heliospheric neutral current sheet to develop a model for the time dependence of ACRs at all radii near the helioequatorial plane. This phenomenological model reproduces the observations at 1 AU, Voyagers 1 and 2, and Pioneer 10 quite well. The model also indicates that the helioequatorial source intensity at the shock varies by a factor of ~ 10 , depending on solar magnetic polarity. The location of the solar wind termination shock during 1980-1990 is found to be ≤ 92 AU, with a best-fit of 84 AU.

1 Introduction:

The termination shock is the source of the anomalous cosmic rays (ACRs) (Pesses et al. 1981), and during the ~ 11 -year period when the Sun's magnetic field direction is inward in its northern hemisphere ("A<0 period"), positively-charged particles are thought to enter the heliosphere by drifting along the heliospheric current sheet (HCS) (Jokipii 1986). The degree of tilt of the HCS might be expected to affect such access, resulting in a relationship between the current sheet tilt and the intensity gradient.

With a positive polarity field (A>0), positively charged particles radially diffuse inward at higher latitudes and drift down to and outward along the current sheet, leading to a different relationship between the radial gradient at low latitudes and the tilt of the current sheet. The observed solar cycle variation of the radial mean free path when A>0 (Cummings & Stone 1999b) suggests that when the current sheet tilt is $\lesssim 35^\circ$, drifts ensure that the radial gradients at lower latitudes reflect the much smaller radial gradients expected at higher latitudes. However, as tilts become larger than $\sim 35^\circ$, drifts are increasingly inhibited and the radial gradients at low latitudes increasingly reflect the much smaller mean free paths expected at low latitudes (see, e.g., Zank et al. (1998)).

The time history of the tilt angle is available from solar magnetic field observations by the Wilcox Solar Observatory (<http://quake.stanford.edu/wso/wso.html>) for each Carrington rotation (~ 27.3 days in duration) from 1976 onward. The HCS is frozen into the expanding solar wind, so that at any given time the tilt values can be visualized as extending from the Sun all the way to the termination shock in a series of "steps", the radial extent of each step being proportional to the solar wind speed. Because of the relationship of the tilt and the particle intensity radial gradients, the radial profile of the tilt translates into a radial profile of the radial gradient. With an assumed ACR source intensity and shock location, the ACR intensity at any position interior to the shock for any given time period can be calculated. Thus the time history of the ACR intensity at the Voyager and Pioneer spacecraft, as well as at 1 AU, can be calculated and compared to the observations. Earlier versions of this approach can be found in Cummings et al. (1994) and Cummings & Stone (1999a).

2 Observations:

The observations of the radial gradient of ACR oxygen from instruments on the Voyager and Pioneer spacecraft around the 1987 solar minimum period are shown as a function of the tilt angle midway between Voyager 2 (V2) and Pioneer 10 (P10) in Figure 1a. At tilt values less than $\sim 25^\circ$, the gradient is essentially proportional to the HCS tilt, as expected for the A<0 period. Above 25° the gradient appears to saturate at ~ 8 %/AU and is no longer sensitive to the tilt. This saturation is probably due to radial diffusion which allows the particles to "short-circuit" the large amplitude waves of the HCS at the larger tilt angles (LeRoux & Potgieter 1992).

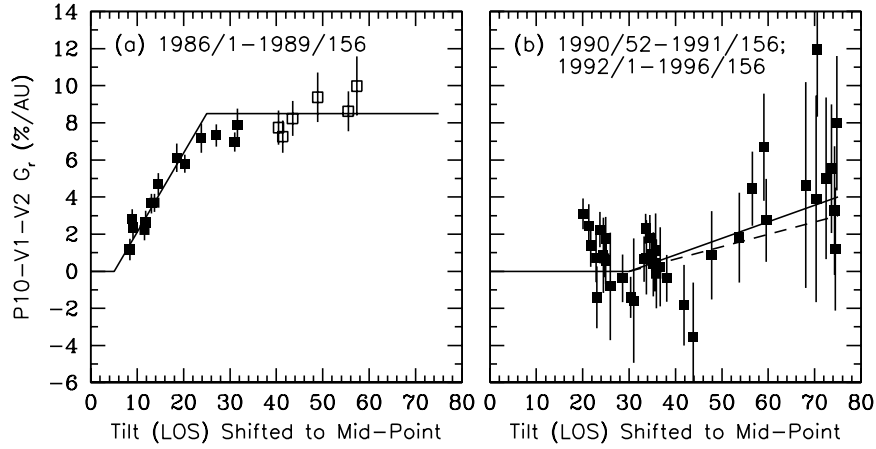


Figure 1: a) The radial gradient of 7.1-17.1 MeV/nuc ACR oxygen between the radial positions of V2 and P10 versus the HCS tilt angle for twenty 52-day periods between 1986/1 and 1989/156 ($A < 0$). The average radial location for these gradients is ~ 33 AU. b) Same as (a) except for the $A > 0$ time period shown. The average radial location is ~ 50 AU. In both panels, the classical, line-of-sight (LOS) tilt angle from the Wilcox Solar Observatory has been convected to the midpoint of V2 and P10 at the solar wind speed appropriate for the individual Carrington rotation. The solid and dashed lines are the $G_r(\text{tilt})$ relationships that will be used later in a model calculation. Reproduced from Cummings and Stone (1999).

For the $A > 0$ period, the gradient vs. tilt relationship in Figure 1b is quite different as expected. The gradients are very small on average when the tilt is $\leq 35^\circ$, increasing for larger tilt angles as particle drift from higher latitude is increasingly inhibited. The variation in the gradients at the highest tilts reflects the increased level of transient perturbations that occur at solar maximum.

The tilt angles necessary for constructing the model are shown in Figure 2.

3 Tilt Model:

To construct the model we use the lines in Figures 1a and 1b instead of the actual data. This permits us to interpolate the gradient for any tilt value. For the $A > 0$ period, there are two lines in Figure 1b: the solid line was used for the period 1990.5-2000.5 and the dashed line was used for the period prior to 1980.5. Note that pre-1980.5, we don't have gradient vs. tilt data to use but assume the relationship is similar, but not exactly the same, as it was in the 1990's. We introduced a radial dependence to the gradient vs. tilt relationship to account for the possibility that the $G_r(\text{tilt})$ relationships shown in Figure 1a, measured at $r_{obs} \sim 33$ AU, and the relationship shown in Figure 1b, measured at $r_{obs} \sim 50$ AU, may scale with radial position. The form of the relationship we used was: $G_r = G_r(\text{tilt})(r/r_{obs})^n$ where n was allowed to vary to best-fit the observations from 1980.5-1990.5.

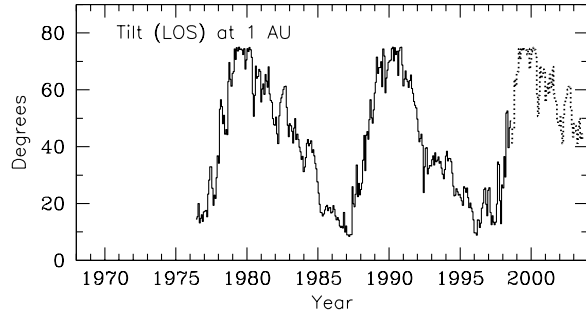


Figure 2: Average tilt angle of the heliospheric current sheet from the classical, line-of-sight data from the Wilcox Solar Observatory. The data have been time-shifted to 1 AU by adding 5 days to the solar observation time. The dotted line is the data from 20 years prior plotted into the future.

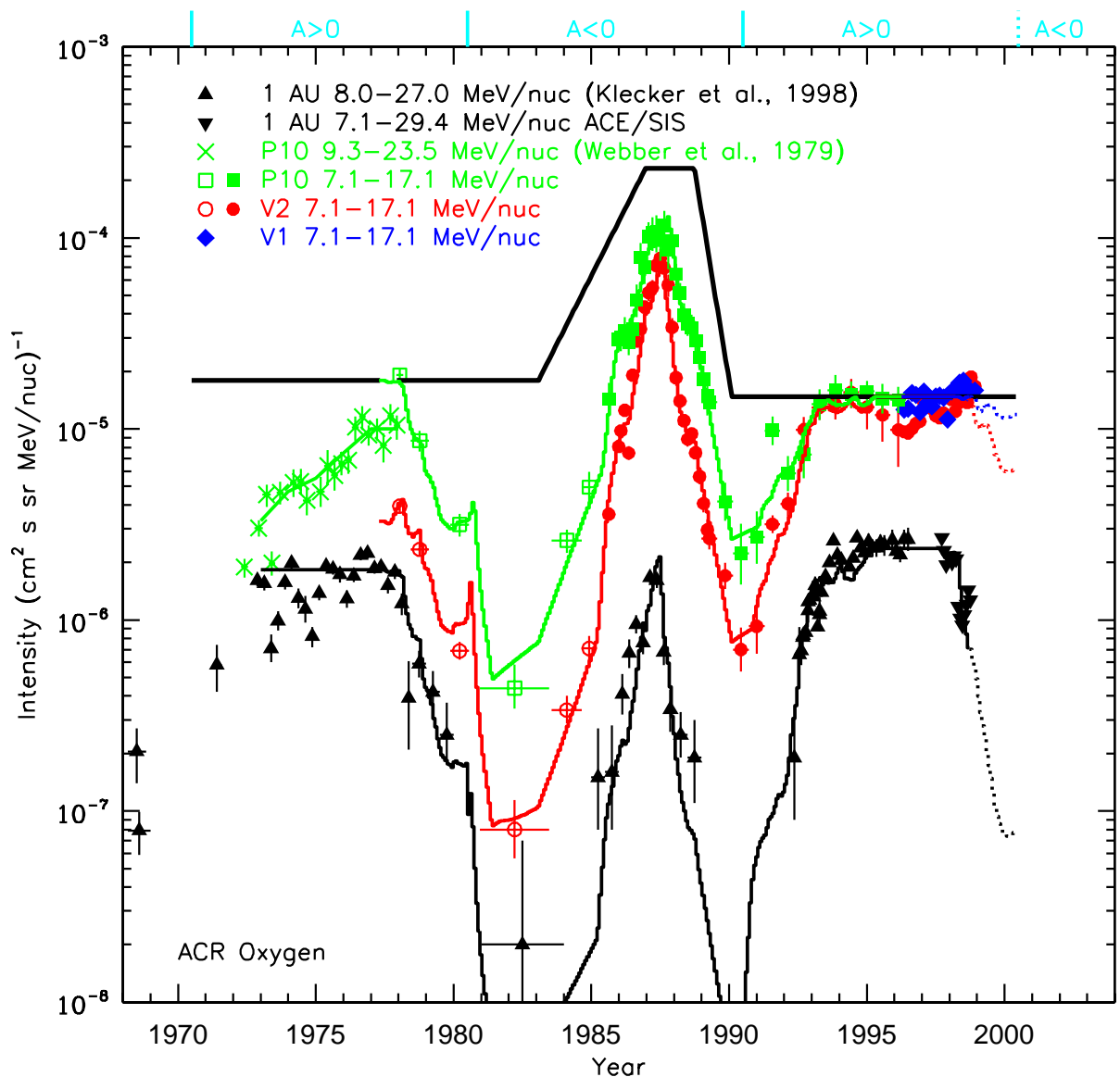


Figure 3: Quiet-time oxygen intensities versus time. The triangles are data from a variety of spacecraft at 1 AU (OGO 5, IMP 6, 7 & 8, and SAMPEX) and are reproduced from Figure 1 of Klecker et al. (1998). The inverted triangles are preliminary data from the SIS instrument on the Advanced Composition Explorer mission. The squares after 1978 are P10 O intensities with 7.1-17.1 MeV/nuc. Prior to 1978, P10 O intensities with 9.25-23.5 MeV/nuc are taken from Webber et al. (1979) and plotted as the crosses. The diamonds are from V1. Filled symbols for Voyager and Pioneer data reflect intensities corrected to the heliographic equator using the measured latitude gradient. The upper solid line is the assumed intensity at the shock in the energy range 7.1-17.1 MeV/nuc. The model calculations for the ACR O intensity at 1 AU, V2, and P10 are shown as the lower set of three curves with 1 AU being the lowest curve, V2 the middle curve, and P10 the upper curve. The 1 AU curve and the P10 curve prior to 1978 have been scaled to the energy range of the observations as described in the text. The dotted portions of the model curves are extrapolations into the future assuming the tilt versus time dependence shown as the dotted curve of Figure 2. The different polarity portions of the solar cycle are marked at the top of the figure. (For an animated version of the model go to http://www.srl.caltech.edu/personnel/ace/tilt_movie_inf.html)

Since most of the observations are near the heliographic equatorial plane, the model reflects intensities of particles at low latitudes. Because the maximum ACR intensity at the shock is expected to move from the heliographic equatorial region to the heliospheric poles as the heliosphere transitions from from $A < 0$ to $A > 0$, we allow the shock intensity (at the helioequator) to vary in a restricted way. We allow an exponential increase with time prior to the maximum intensity in 1987 and an exponential decrease thereafter. The transition times are varied to provide the best match to the observations. Three plateau intensities at the shock are allowed, one for each portion of the solar cycle (first $A > 0$, $A < 0$, and final $A > 0$). We fixed the solar wind speed at 440 km s^{-1} which implies that each Carrington-rotation tilt observation corresponds to 6.93 AU in radial range.

We found that the model with the parameters listed above reproduced the observations in the outer heliosphere quite well but needed an additional feature to match the 1 AU observations. The feature is a fixed gradient (somewhat different for each polarity portion of the solar cycle) inside 11.4 AU. This gradient was fixed in two steps, in accordance with the observations in the late 1970's (Webber et al. 1979). From 1 to 4.5 AU for the periods 1970.5-1980.5, 1980.5-1990.5, and 1990.5-2000.5, the fixed gradients (in %/AU) were 25.0, 47.6, and 25.1, respectively. From 4.5 to 11.4 AU, for the same three periods, the fixed gradients were 12.0, 11.4, and 5.4, respectively. Additionally, the maximum gradient beyond 11.4 AU was limited to these values from 4.5 to 11.4 AU.

4 Discussion:

Figure 3 shows the results of the model and the observations at 1 AU and at the radial positions of V2 and P10 (and at V1 after mid-1996 when P10 ceased returning data). In Figure 4 we show the dependence of the best-fit shock locations on the parameter n , which scales the gradient vs. tilt relationship. For reasonable values of this parameter, 0 to -1, the shock location is constrained to be ≤ 92 AU, with a best-fit value of 83.7 AU for $n = -0.82$.

Acknowledgments: We thank W. Webber for providing P10 data. We thank the Wilcox Solar Observatory for the tilt data obtained through their website. We thank the ACE/SIS team for the ACR O intensities. This work was supported by NASA under contract NAS7-918.

References

- Cummings, A. C. & Stone, E. C. 1999a, *Adv. Space Res.*, in press
 Cummings, A. C. & Stone, E. C. 1999b, in *Proc. 26th Internat. Cosmic Ray Conf.*, SH 4.2.03, Salt Lake City
 Cummings, A. C., Stone, E. C., & Webber, W. R. 1994, *J. Geophys. Res.*, 99, pp. 11547–11552
 Jokipii, J. R. 1986, *J. Geophys. Res.*, 91, pp. 2929–2932
 Klecker, B., Mewaldt, R. A., Bieber, J. W., et al. 1998, *Space Sci. Rev.*, 83, pp. 259–308
 LeRoux, J. A. & Potgieter, M. S. 1992, *Astrophys. J.*, 390, pp. 661–667
 Pesses, M. E., Jokipii, J. R., & Eichler, D. 1981, *Astrophys. J. Lett.*, 246, pp. L85–L89
 Webber, W. R., McDonald, F. B., Trainor, J. H., et al. 1979, in *Proc. 16th Internat. Cosmic Ray Conf.*, 5, pp. 353–356, Kyoto
 Zank, G. P., Matthaeus, W. H., Bieber, J. W., et al. 1998, *J. Geophys. Res.*, 103, pp. 2085–2097

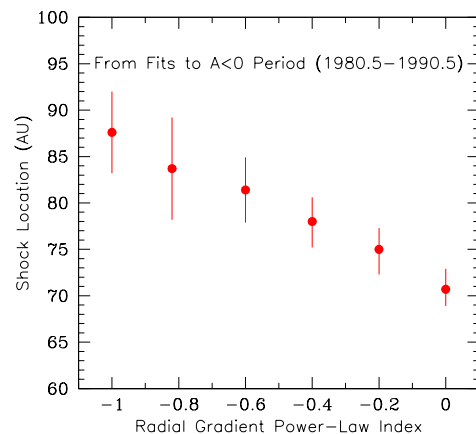


Figure 4: The best-fit shock location (from 1980.5-1990.5 data) vs. the assumed value of the power-law index n in $G_r = G_r(\text{tilt})(r/r_{\text{obs}})^n$